Engineering and Technology Journal
Journal homepage: https://etj.uotechnology.edu.iq

Experimental Study of F2833x/Texas Ins. for Constructing Speed Controller on a Synchronous Motor Based on SVPWM Method

Enas D. Hassan[a], **Inaam I. Ali** [b], **Khalid G. Mohammed**[c*]

[a,c] Electrical Power and Machine Engineering Dept., College of Engineering, University of Diyala, Diyala Province, Iraq.
[b] Electrical Engineering Dept, University of Technology-Iraq, Alsina'a Street, 10066 Baghdad, Iraq.
*Corresponding author Email: khalid_alkaisee@engineering.uodiyala.edu.iq

HIGHLIGHTS

- The directional inclusion method was used to implement the six inverter switches (IGBTs) mechanism.
- Mathematical calculations were made for Space Vector Pulse Width Modulation (SVPWM) method.
- The experimental board Voltage Source inverter (VSI) was tested extensively

ARTICLE INFO

Handling editor: Ivan A. Hashim

Keywords:
DC/AC Inverter; TMS320f28335; SVPWM; Induction Motor

ABSTRACT

Microprocessor programming algorithms in electrical inverter drive systems are essential in developing and formulating modern methods in closed control circuits. The microprocessor used in the current research, TMS320f28335, has a high system clock s frequency (150 MHz) that reaches up to, which gives an almost perfect ability to output the three-voltage sinewave generated from the inverter under consideration. Obtaining a sinewave voltage means the lowest possible harmonics (THD) and thus the best performance of the induction motor at starting and dynamic stability. The current research used the directional inclusion method to implement the six inverter switches (IGBTs) mechanism. Mathematical calculations were made for Space Vector Pulse Width Modulation (SVPWM) method, and then the microprocessor was programmed to implement it. The practical board Voltage Source inverter (VSI) was tested extensively.

1. Introduction

Inverters are widely used in a variety of power applications. In the last decade, there has been a significant development in the control mechanism of power electronics such as IGBT, MOSFET, and BJT coincided with the development of modern advanced control units such as digital signal processors (DSP) [1]. Originally, an inverter is a transformer whose function is to convert the DC voltage of many generation sources into AC voltage for efficient transmission and distribution. Inverters are classified into voltage source inverters (VSI) and current source inverters (CSI). The voltage source inverter has a low input impedance, while the current inverter has a high input impedance [2]. During VSI, the output voltage waves are not affected by the load, and the output current waves of the CSI are not affected by the load. Voltage source inverters are used in applications requiring constant voltage, while current source inverters are best for applications requiring constant current. Therefore, more importance was given to voltage source inverters. The main reason VSI is important is its ability to convert high voltages with low harmonics contents. Hence, VSI controls AC motors due to the rapid development of power electronics technologies. Variable voltage and frequency inverter motors are two of the most important methods used to control the speed of induction motors common in industries. VSI receives constant voltage from a source such as a DC source and is converted into an alternating current voltage source with variable frequency and amplitude. VSI is controlled by various technologies, including PWM [3][4].

PWM technology is the most efficient and most used inverter control technology as it does not require any additional components. With PWM technology, one can obtain the appearance of the output wave by changing the switching time. The output voltage is based on eight different states' DC conduction voltage settings. The wave width modulation diagram has different methods like the sine pulse width modulation (SPWM) method, square wave modulation method, space vector pulse width modulation (SVPWM) method, etc. These various methods are used in energy applications [5] [6]. The three-phase voltage source inverter consists of six switching devices, as shown in Figure 1. The present paper introduces an experimental

http://doi.org/10.30684/etj.v40i2.2171
Received 18 May 2021; Accepted 1 July 2021; Available online 25 February 2022
2412-0758/University of Technology-Iraq, Baghdad, Iraq

device that controls the speed of the three-phase induction motor to be constant with varying different loads imposed on the shaft of the motor. The microprocessor TMS320f28335 is equipped with a control algorithm that manages the SVPWM technology for the six in the inverter Inverters need a gate drive circuit to operate the power electronics switches. The gate drive circuit is an important and integral part of the ECT system, connecting the power transistor to the microcontroller. Therefore, the design of the gate drive circuit is strongly related to the output efficiency and the reliability of the inverter / converter decision as the output of the inverter mainly depends on the driving of the gate driver circuit. Poor driver operation or wrong choice of driver may result in the designed inverter output not according to requirements [8]. Low-power applications often require a reliable, cost-effective, and successful driver design for power applications. Therefore, gate driver circuits are vital in the design of power electronics inverters. Their function is to operate power semiconductor devices (IGBTs, MOSFETs, and SIC transistors) and have high output voltages and amperages with a gate drive circuit voltage that may normally reach 36 volts. There are various types of gate circuits for MOSFET, IGBT, and SIC-MOSFET. The majority of the classes of gate actuating circuits are estimated according to the configuration, with the amount of DC power supply, gate motor power, and power transistor assembly class, simultaneously to determine the maximum value of the output voltage and current [9]. In this paper, a gate drive circuit was designed to drive the IGBTs to a three-phase inverter consisting of three arms. Each arm contains two switches i.e., the inverter consists of six IGBT switches used to control a three-phase induction motor, with a DC connection voltage of up to 36 volts. The three-phase inverter was controlled using space vector pulse width modulation (SVPWM) technology. The main characteristic of using SVPWM technology is that the DC correlation can be used to the highest value compared to SPWM technology and the harmonic content is lower. The SVPWM signals are generated by the

2. Space Vector Pulse Width Modulation (SVPWM)

SVPWM is a direct digital technology that Holtz and van der Brock first introduced in 1982. It is a type of pulse width modulation (PWM). SVPWM has become commonly used in three-phase Voltage Source Inverters (VSI) in industrial applications, especially for controlling AC induction motors [5][10]. Space vector pulse width modulation (SVPWM) is a modified switching technique, as shown in Figure 2. It represents the conversion of a three-phase voltage system into a two-way voltage system in orthogonal coordinates. The SVPWM concept focuses on generating a rotating magnetic field of constant size, as shown in Figure 3 for the stator windings of the three phases of the machine, which should also be commendable by the processor to deal with it in real-time to modify the inverter output voltage [11]. The goal of SVPWM is to become a three-phase sine wave format with respect to time on the three axes that are shifted over time by 120 ° from each other, resulting in a space vector with constant amplitude rotating at a constant velocity. Furthermore, by using two-phase voltage elements, the inverter output is easy to adjust.

SVPWM technology has higher output voltages for the same DC bus voltage, lower switching losses, and better harmonic performance [13]. In the case of the SVPWM mechanism, the six-switch three-phase inverter comprises the output of eight vectors, two zero vectors, as shown in Figure 3. At the same time, six active conductors (V1 to V6) form a regular hexagon, the field between the six vectors into equal six sectors to produce the reference voltage (V_{ref}) sampled one time for each sub-cycle Ts. The zero vector of the hexagon V_0 is in the middle. To produce the reference voltage V_{ref} that is sampled once per *Ts* sub-cycle. Classic SVPWM uses a transposition sequence that divides the timing of the zero vector evenly into two states of zero in each sub-cycle [14][15]. The PWM space vector technology and the eight vectors are shown in Figure 3.

3. Mathematical Model of SVPWM

The model of three-phase VSI that shown in Figure 1. As shown beneath, S_1 to S_6 are the six power switches that are operated to find the output and have eight allowable switching states (000-111). *Va*, *Vb,* and *Vc* represent the voltages coming from the inverter. The six switches devices that make up the output are controlled through a, a', b, b', c, and c'. While upstairs, the switches are running (while a, b or c is 1), the opposite, a lower switch is shut down (the corresponding a', b' or c' is 0). For this, the on and off states of the upper side switches S1, S3, and S5, or their substitutions in the case of a, b, and c, are used to determine the output voltage [16].

The relationship amidst the switching variable vector [a, b, c]t and the line-to-line output voltage vector [Vab Vbc Vca]t and the phase (line-to-neutral) output voltage vector [Van Vbn Vcn] is obtained during equations 1 and 2.

Where Vdc is the DC supply voltage. Equations 1 and 2 show the three-phase voltages at the output of the inverter which applied to motor windings, as shown in Figure 1. Also, the matrices elements in the above equations can be obtained according to the equations below (3, 4, and 5).

As shown in Figure (3) above, thither are eight probable groups of on and off states of the upstairs switches. Table (1) shows the eight states and the resulting line-to-line voltage and phase voltage according to (1) and (2). By applying the idea of the space vector and the transformation method of the three axes, the desired output voltage is obtained on the desired reference voltage vector, approximately Vref, in the frame d-q, where the average output voltage is generated on the inverter for a short period T, similar to the reference voltage Vref, during about the same time. It is the goal of SVPWM theory. Using this technology, a Field Oriented Control motor speed control system is developed based on the TMS320F28335 microprocessor.

$$\begin{bmatrix} Vab \\ Vbc \\ Vca \end{bmatrix} = Vdc \begin{bmatrix} 1 & -1 & 0 \\ 0 & 1 & -1 \\ -1 & 0 & 1 \end{bmatrix} \begin{bmatrix} a \\ b \\ c \end{bmatrix} \quad (1)$$

$$\begin{bmatrix} Van \\ Vbn \\ Vcn \end{bmatrix} = \frac{1}{3} Vdc \begin{bmatrix} 2 & -1 & -1 \\ -1 & 2 & -1 \\ -1 & -1 & 2 \end{bmatrix} \begin{bmatrix} a \\ b \\ c \end{bmatrix} \quad (2)$$

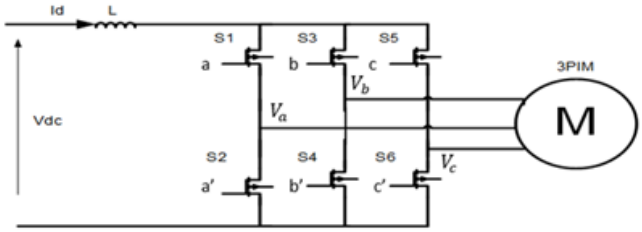

Figure 1: Three-Phase Voltage Source Inverter Configuration

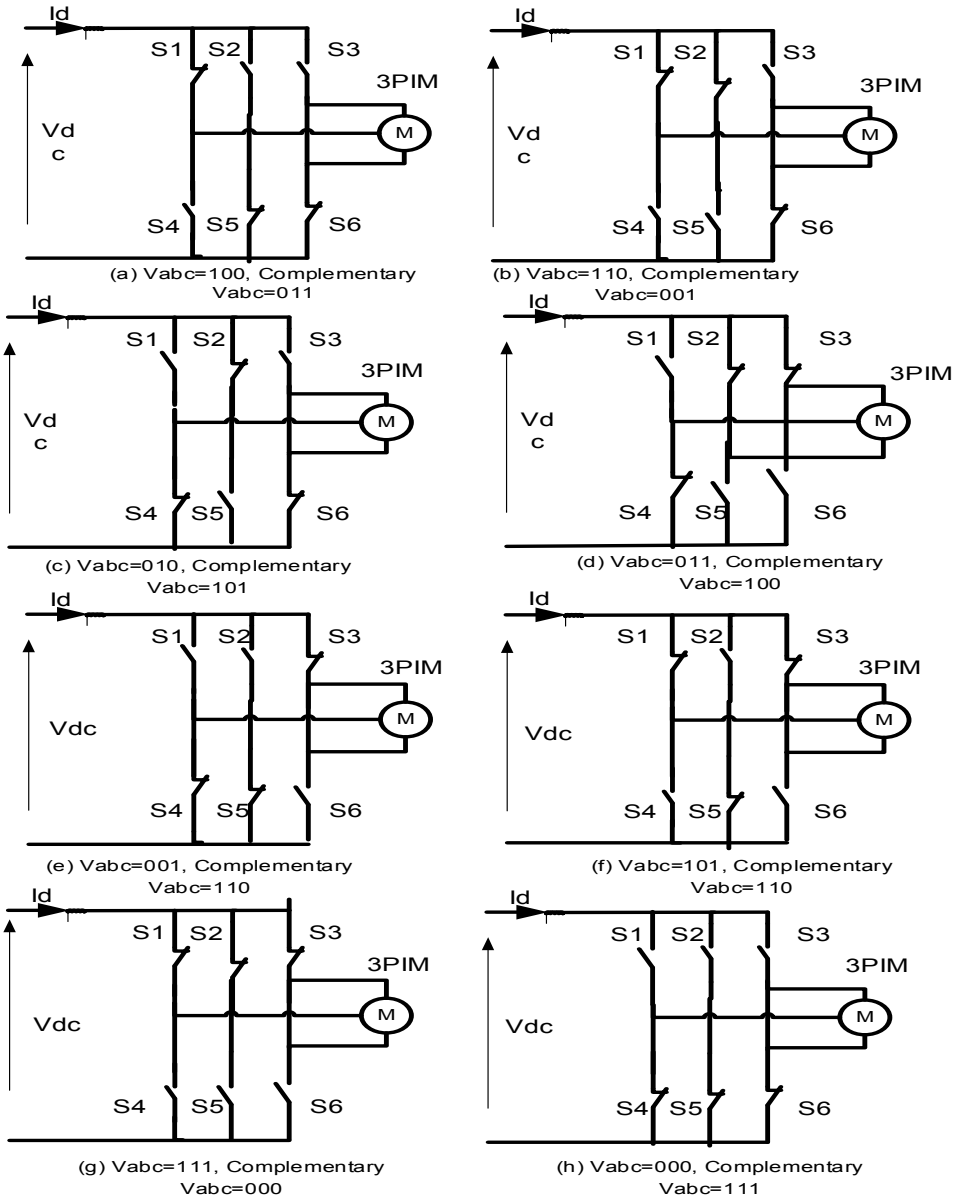

Figure 2: Three-phase VSI output voltage vectors and their sectors of rotating flux and power on-off switches sequentially [12]

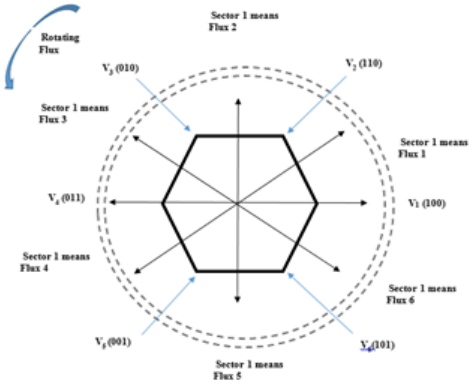

Figure 3: Space vector PWM technique [13]

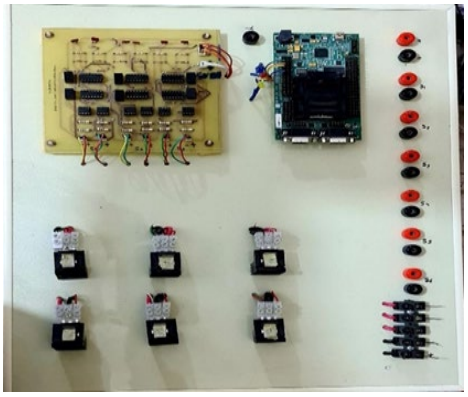

Figure 4: Speed controller kit

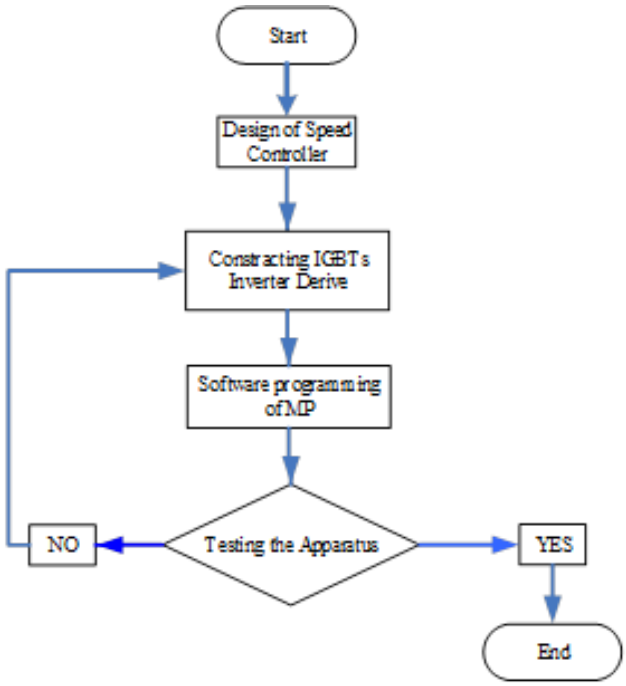

Figure 5: Flowchart displays the sequence of operations in the control kit

4. Implementation of the space vector PWM

The following steps explain the implementation of the SVPWM technique:

1- Determining V_d, V_q, V_{ref}, and angle (α).

2- Determining the time duration T_1, T_2, and T_o.

3- Determining the switching time T_s for every switch's device (S1 to S6).

To understand the SVPWM technique, the three-phase voltage (3) to (5) is represented by the abc reference frame form with two d, q coaxial frames to implement the SVPWM. (d) refers to the horizontal axis and (q) the vertical axis, as shown in Figure 5. The equations below show the balanced three-phase voltages [2, 4, 6, 7].

$$Van = Vm \sin(2\pi ft) \tag{3}$$

$$Vbn = Vm \sin\left(2\pi ft - \frac{2\pi}{3}\right) \tag{4}$$

$$Vcn = Vm \sin\left(2\pi ft + \frac{2\pi}{3}\right) \tag{5}$$

By applying Park's transformation technique during the rotating reference scope, the d, q reference scope is as illustrated below by (6) to (9) [4].

$$Vd = \frac{2}{3}(Va\cos 0 + \text{Vb}\sin\frac{2\pi}{3} + Vc\ sin\frac{4\pi}{3}) \ = Va - \frac{1}{2}Vb - \frac{1}{2}\text{Vc} \quad (6)$$

$$Vq = \frac{2}{3}(Va\sin 0 + Vb\sin\frac{2\pi}{3} + Vc\ sin\frac{4\pi}{3}) \quad (7)$$

$$Vq = \frac{\sqrt{3}}{2}\ Vb - \frac{\sqrt{3}}{2}Vc \quad (8)$$

$$\begin{bmatrix} Vd \\ Vq \end{bmatrix} = \begin{bmatrix} 1 & -\frac{1}{2} & -\frac{1}{2} \\ 0 & \frac{\sqrt{3}}{2} & -\frac{\sqrt{3}}{2} \end{bmatrix} \begin{bmatrix} Va \\ Vb \\ Vc \end{bmatrix} \quad (9)$$

The reference voltage (V_{ref}) is calculated using (10).

$$|Vref| = \frac{2}{3}\ \alpha\sqrt{Vd^2 + Vq^2} \ = \text{V}_1\text{T}_1 + \text{V}_2\text{T}_2 + \text{V}_z\text{T}_z \quad (10)$$

The angle for the Vref (α) is identified by (11) [7].

$$\alpha = tan^{-1}(\frac{Vd}{Vq}) \ = 2\pi ft = \omega t \quad (11)$$

Where *f* is the fundamental frequency.
Step 2- Determining the time duration T_1, T_2, and T_0.
Through Figure (1), the time for switching during every sector can be limited as shown:

$$T_1 \ = \frac{\sqrt{3}\ \text{Ts}\ |\text{Vref}|}{\text{Vdc}}\ (\sin(\frac{\pi}{3} - \alpha + \frac{(n-1)\pi}{3}) \quad (12)$$

$$T_2 \ = \frac{\sqrt{3}\ Ts\ |Vref|}{Vdc}\ (\sin(\ \alpha - \frac{(n-1)\pi}{3}) \quad (13)$$

$$T_0 = \ Ts - T_1 \ - T_2 \quad (14)$$

$$Ts = \frac{1}{fs} \quad (15)$$

Where n is the number of sectors, Ts is the switching period.

5. DSP TMS320F28335 Controller board for SVPWM

Digital control using a DSP microprocessor gives system performance precision, optimization, and real-time execution. The TMS320 family of digital signal processors is introduced and is a more extensive choice of other digital signal processors to suit special application needs [17]. In 1982, the first single-chip DSP was released by Texas Instruments. It provided designers with support and complementary technology by equipping them with advanced next-generation systems. Texas Corporation developed TMS320F28335 clusters with DSP that deliver high system performance and accuracy. The DSP TMS320F28335 series includes peripherals on the control panel such as 88 general-purpose ports for GPIOs used to implement I/O signals and converters for analog to digital (A/D), and digital to analog (D/A) high speed and flash memory (SRAM) that are used when the digital signal processor is connected to a specific program on a calculator such as CCS [18]. It also contains the CAN array, output logic, and PWM circuit, including six ePWM units responsible for generating the PWM signal required for the application and the encoder used for the engine control function. DSP TMS320F28335 programmed by code composer studio in C / C ++ language or using Matlab / Simulink software. DSP TMS320F28335 has a 32-bit CPU that includes an 8-stage matrix frame, and this distinguishes the CPU in its ability to apply 8 directions simultaneously for one system hour. 32-bit floating-point unit, 256KB SRAM, 512KB flash memory, 30MHz input clock, and popular USB JTAG controller interface that support real-time error handling with JTAG support, with user ability to handle memory periods and records without downtime processing [19][20]. The current research whole apparatus (speed controller kit), as explained in Figure 4, mainly consists of Microprocessor Texas TMS320f28335, power electronic Drive the alignment between the microprocessor and the voltage source inverter, Electronic switches which are six IGBTs, Encoder and tested three-phase motor

6. Algorithm of TMS320F28335 with SVPWM

1- Calculation of (T_a,T_b,T_0) as the example below are applied normally by using a software program for all periods at rest time using (12), (13), and (14) over sequential periods from one to six sectors and their subsectors [4].

2- The estimated data are being temporarily stored in EPROM. Then the data has been transferred to the IGBTs gates. In the beginning, the periods (T_a,T_b,T_0) for each sector start using sub-sector equal steps (10 °) starting from θ = 10°, 20°, 30° ...., 350°). Because the periods (T_a,T_b,T_0) are identical between the six sectors, the calculations for a single sector can be implemented as shown below [2, 4, 9]. An initial description of the sequence of operations in the control kit can be described in the flowchart as clarified in Figure 5.

$$\text{T}_{\text{sector}} = \frac{T_{rated}}{m} = \frac{1/50Hz}{0.9} = \frac{0.02}{0.9} = 0.0222 \text{ sec.}$$

$$T_{ssector} = \frac{T_{sector}}{6} = \frac{0.0222}{6} = 0.0037 \text{ sec.}$$

$$T_s = \frac{T_{ssector}}{6} = \frac{0.0037}{6} = 0.000617 \text{ sec. (for 90\%)}$$

Similarly (T_s) of 80% rated voltage is:

$$T_s = \frac{T_{sector}}{6} = \frac{0.00416}{6} = 0.000694 \text{ sec. (for 80\%)}$$

The proposed motor speed control system is developed based on the control algorithm of the DSP TMS320F28335 with SVPWM by employing Composer Studio (CCS) software. The control system takes the speed reference signal is input through the speed control algorithm. This feedback signal is used for reference correction of the speed during turbulence on the motor, such as the change in mechanical load. Therefore, the difference between the reference speed and the real speed will increase. The PI controller is a good choice for detecting speed errors. These signals are converted into stationary reference frame voltages and produce an optimal duty cycle of the PWM control signal. SVPWM technology takes three input values and produces six pulse width adjustments of a three-phase inverter IGBT consisting of six IGBTs used to control a three-phase induction motor. The flowchart in Figure 5 shows the motor speed control assembly sequence of operations.

7. Results and Discussion

The experimental results are obtained by implementing the practical experiment of the speed controller kit (of the gate drive circuit that designed to drive the IGBTs to a three-phase inverter using the TMS320F28335 microprocessor), as explained in Figure 4 to control of 3-phase induction motor based on the constant velocity with variable mechanical load states. PWM pulses are generated via the SVPWM process, which includes obtaining a reference voltage by simplifying the state of the SVM. Table 1 and Figures 6, 7, 8, 9, and 10 show the system's speed response to the control scheme and the difference in the duty cycles of the pulses modified under the different loads placed on the motor shaft because the controller changes the duty cycle of the control signal in the PWM to obtain the required speed. The set of speed controllers used to keep the shaft speed constant at 360 rpm adjusted the duty cycles during the five test phases.

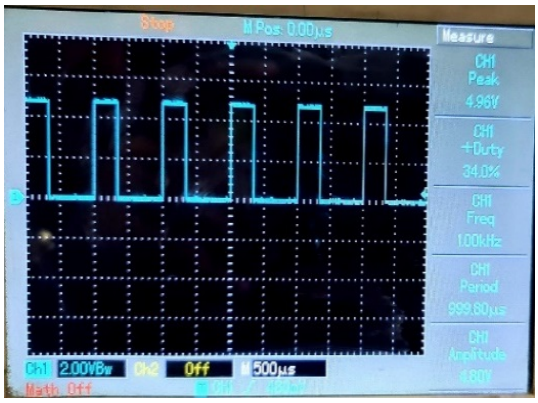

(a) Phase-A PWM

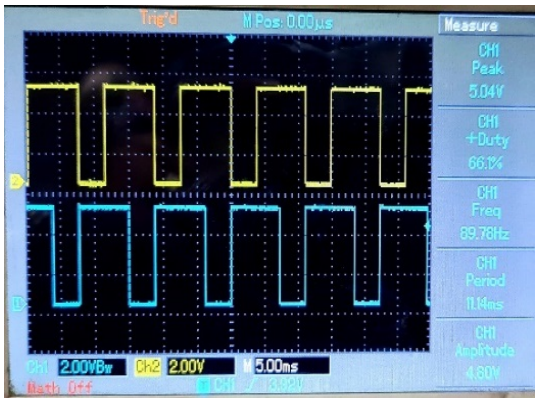

(b) Phase operating pulses (Invers phases A and B)

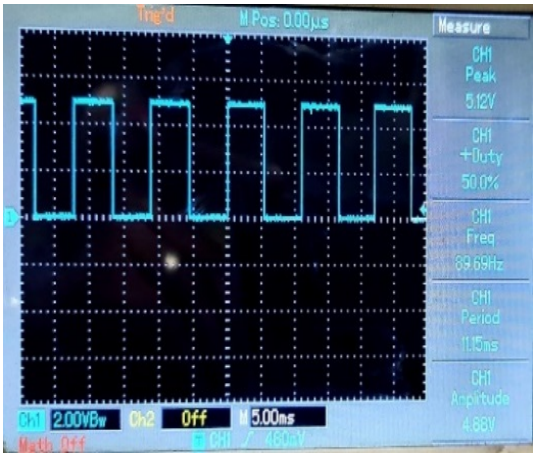

(c) Speed sensor pulses

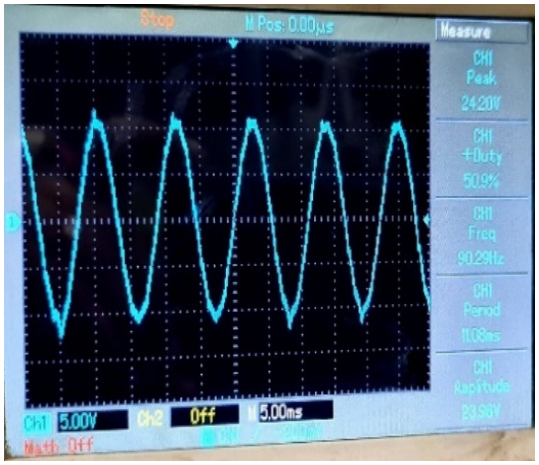

(d) The Sine waveform of the reference voltage of phase-delivered to 3PIM.

Figure 6: Test 1, Experimental results of speed response at the steady-state operation under no-load condition

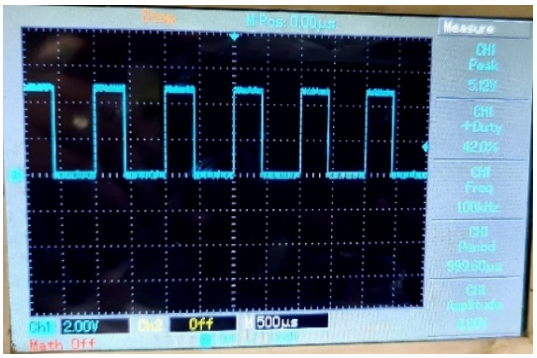

(a)Phase-A PWM

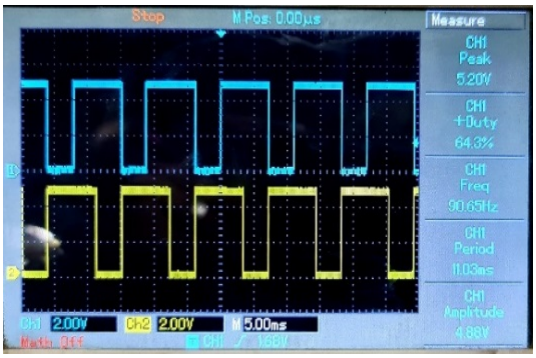

(b) Phase operating pulses (Invers phases A and B)

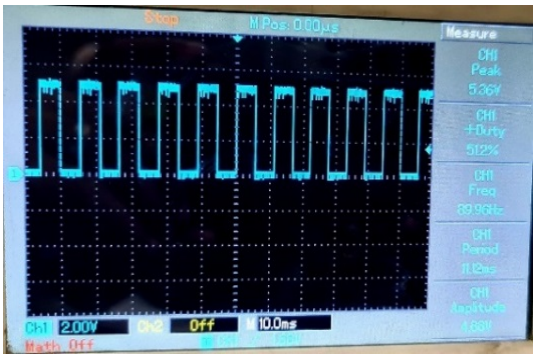

(c) Speed sensor pulses

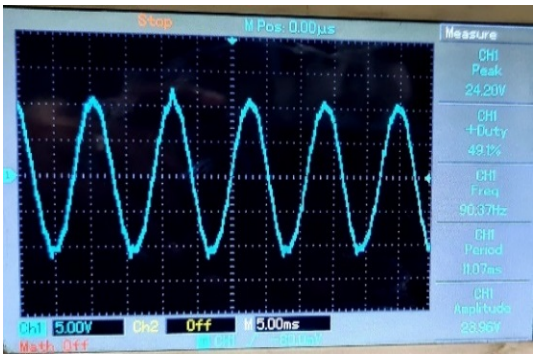

(d) The Sine waveform of the A-phase reference voltage delivered to 3PIM

Figure 7: Test 2, Experimental results of speed response under load 1 condition

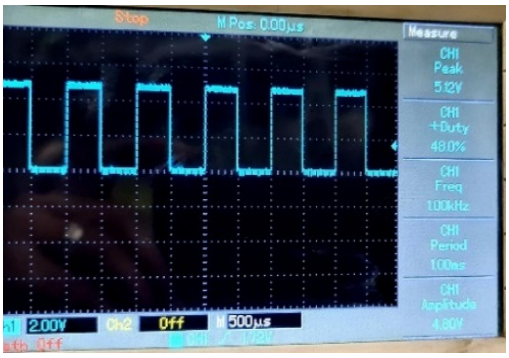

(a) Phase-A PWM

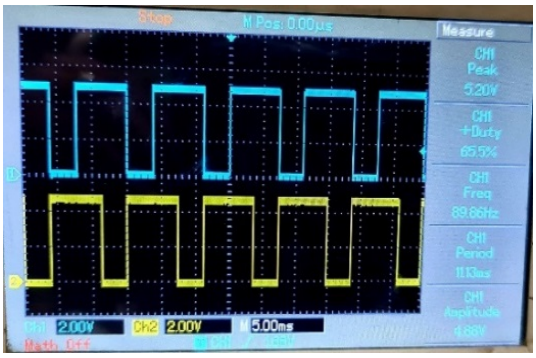

(b) Phase operating pulses (Invers phases a and b)

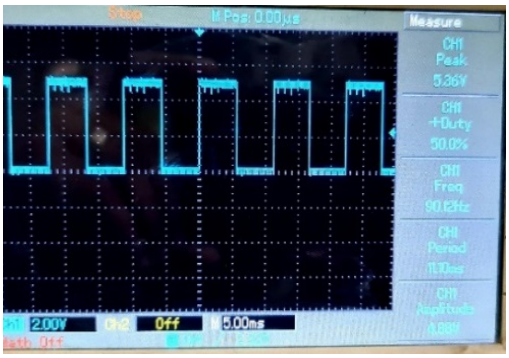

(c) Speed sensor pulses

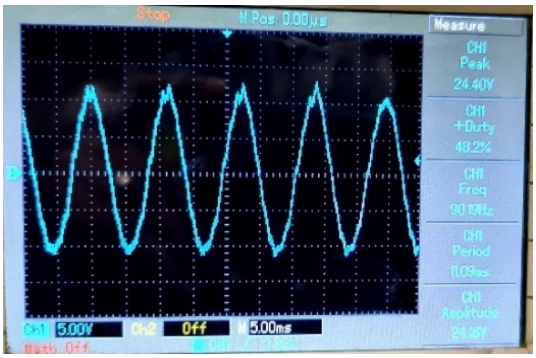

(d) The Sine waveform of the A-phase reference voltage delivered to 3PIM.

Figure 8: Test 3, Experimental results of speed response under load 2 condition

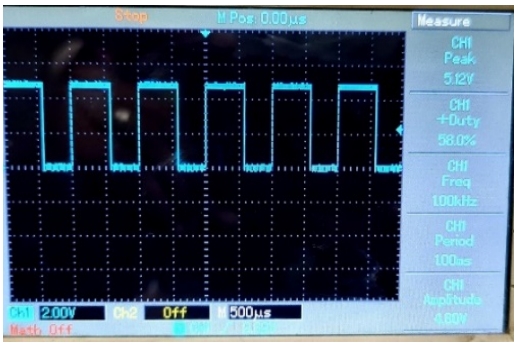

(a) Phase-A PWM

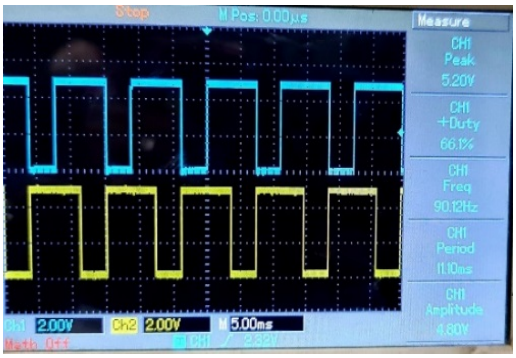

(b) Phase operating pulses, Invers phases a and b

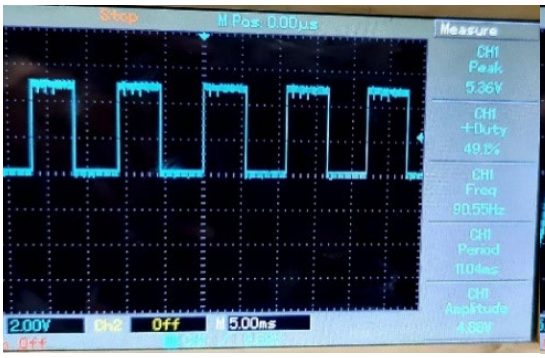

(c) Speed sensor pulses

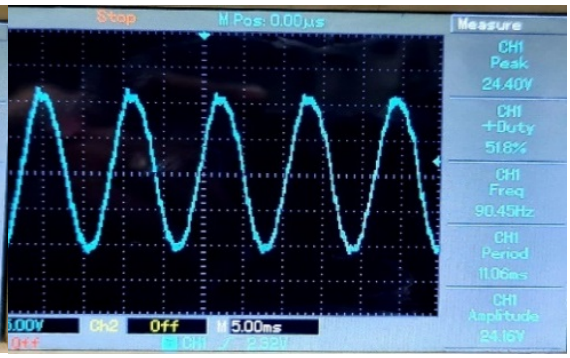

(d) The Sine waveform of the A-phase reference voltage delivered to 3PIM.

Figure 9: Test 4, Experimental results of speed response under load 3 condition

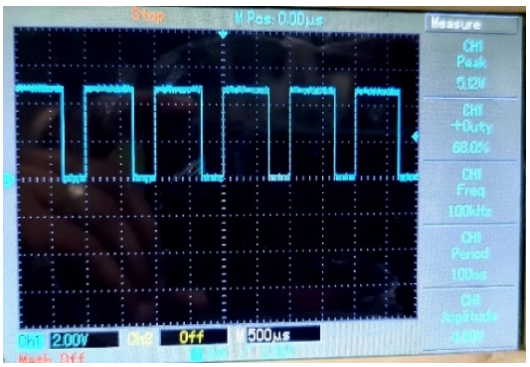

(a) Phase-A PWM

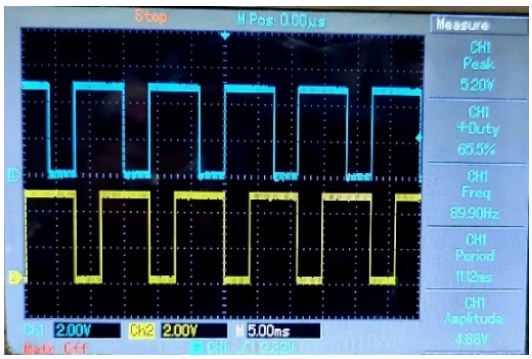

(b) Phase operating pulses, Invers phases a and b

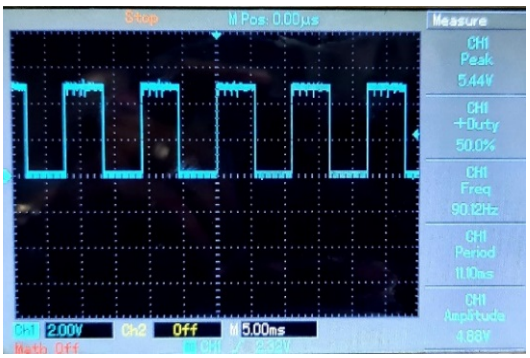

(c) Speed sensor pulses

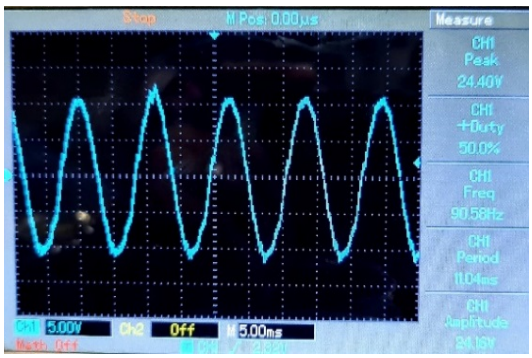

(d) The Sine waveform of the A-phase reference voltage delivered to 3PIM

Figure 10: Test 5, experimental results of speed response under load 4 condition

Table 1: Practical results are drawn current as torque with the speed of a three-phase induction motor with controller

No. Test	Current (Amp)	Duty Cycle %	Speed(rpm)
1	0.4	34 , Vamp=5 V	360
2	0.6	42 , Vamp=5 V	360
3	0.8	48 , Vamp=5 V	360
4	1	58 , Vamp=5 V	360
5	1.2	68 , Vamp=5 V	360

1. Without Load -Test 1 as shown in Table 1 and Figure 6: The first case shows the normal operation of the motor at 360 rpm without load when the motor shaft is free, as shown in Table 1, where we notice that the pulse value is around 34% and the current drawn is within 0.4 Amp.
2. Under Load-Test 2 as shown in Table 1 and Figure 7: It is noticed here that in the case of increase the mechanical load on the motor shaft, as shown in Table 1, the value of the current drawn, which reached 0.6 amperes, means, an increase of 150% compared with the no-load test as explained in Test 1. Therefore, to maintain the speed of the shaft at 360 rpm, the controller has modified the duty cycle to 123% compared to that in the no-load test.
3. Under load-Test 3 as shown in Table 1 and Figure 8: It is noticed here that in the case of increase the mechanical load on the motor shaft, as shown in Table 1, the value of the current drawn, which reached 0.8 amperes, means, an increase of 200% compared with the no-load test as explained in Test 1. To maintain the speed of the shaft at 360 rpm, the controller has modified the duty cycle to 140 % compared to that in the no-load test.
4. Under Load Test 4, as shown in Table 1 and Figure 9: It is noticed here that in the case of an increase in the mechanical load on the motor shaft, as shown in Table 1, the value of the current drawn reached 1 ampere. This means an increase of 250% compared with the no-load test, as explained in Test 1. To maintain the speed of the shaft at 360 rpm, the controller has modified the duty cycle to 170 % compared to that in the no-load test.
5. Under Load -Test 5 as shown in Table 1 and Figure 10: It is noticed here that in the case of increase the mechanical load on the motor shaft, as shown in Table 1, the value of the current drawn, which reached 1.2 amperes, that means, an increase of 300% compared with the no-load test as explained in Test 1. To maintain the speed of the shaft at 360 rpm, the controller has modified the duty cycle to 200 % compared to that in the no-load test.

8. Conclusions

In this study, implementation of hardware Microprocessor algorithm TMS320F28335 was conducted through employing Code Composer Studio (CCS) software for Field Oriented Control with SVPWM technology of 3-phase induction motor based on the constant velocity with variable mechanical load states. During the practical experiment, it is evident from the test results in Table 1 that the speed control toolkit used to maintain constant motor shaft speed with variable mechanical loads has achieved the desired goal of the presented research. The five tests started from the non-load condition as in the first table, where we note that increasing the loads leads to higher values of the drawn currents (0.4, 0.6, 0.8, 1, 1.2) amperes. In other words, it is observed that the gradual increase in the duty cycle of the square wave generates the width (34, 42, 48, 58, 68)% proportional to the increase in the load value. Thus, the motor's stability of the shaft speed was kept constant (360 rpm) Despite these changes in different loads.

Author contribution

All authors contributed equally to this work.

Funding

This research received no specific grant from any funding agency in the public, commercial, or not-for-profit sectors.

Data availability statement

The data that support the findings of this study are available on request from the corresponding author.

Conflicts of interest

The authors declare that there is no conflict of interest.

References

[1] K. T. Maheswari, R. Bharani Kumar, D. Lavanya, S. Boopathimanikandan, Design of SVPWM based Closed-Loop Control of Voltage Source Inverter Fed Induction Motor Drive with PID Controller, Int. Conf. Inventive Syst. Control., (2020) 487–492. http://dx.doi.org/10.1109/ICISC47916.2020.9171181

[2] M. A. Hannan, J. A. Ali, A. Mohamed, M. N. Uddin, A Random Forest Regression Based Space Vector PWM Inverter Controller for the Induction Motor Drive, IEEE. Trans. Ind. Electron., 64 (2017) 2689–2699. http://dx.doi.org/10.1109/TIE.2016.2631121

[3] P. Suresh, L. A. Pothana, M. V. Penmetsa, S. T. Sunkavalli, Speed control of induction motor using spwm based multilevel inverter and parallel converters, Int. J. Recent .Technol. Eng., 8 (2019) 2277-3878. http://dx.doi.org/10.35940/ijrte.B1296.0982S1119

[4] F. A. Hassan, Field Oriented Control For Three Phase Induction Motor Based On Full Neural Estimator And Controller, Eng. Technol. J., 28 (2010) 5014-5027.

[5] E. Nandhini , A. Sivaprakasam, A Review of Various Control Strategies Based on Space Vector Pulse Width Modulation for the Voltage Source Inverter, IETE J. Res., 68 (2020) 3187-3201. http://dx.doi.org/10.1080/03772063.2020.1754935

[6] F. A. Hassan, L. J. Rashad, Particle swarm optimization for adapting fuzzy logic controller of SPWM inverter fed 3-phase I.M, Eng. Technol. J., 29 (2011) 2912-2925.

[7] M. K. Al-Khatat, F. A. Hassan, Modeling and Implementation of Space Vector PWM Driver of 3-Phase Induction Motor, Eng. Technol. J., 27 (2009) 2113-2131.

[8] M. J. Mnati, A. H. Ali, D. V. Bozalakov, Sh. Al-Yousif, A.V. Bossche, Design and Implementation of a Gate Driver Circuit for Three-Phase Grid Tide Photovoltaic Inverter Application, IEEE. Conf. Renew. Energy. Res. Appl., 5 (2018) 701–706. http://dx.doi.org/10.1109/ICRERA.2018.8566923

[9] B. Bhutia, S. M. Ali, N. Tiadi, Design of Three Phase PWM Voltage Source Inverter For Photovoltaic Application, Int. J. Innov. Res. Electr. Electron. Instrum. Control. Eng., 2 (2014) 2321–2004.

[10] H. Mikhael, H. Jalil, I. Ibrahim, Speed Control of Induction Motor using PI and V/F Scalar Vector Controllers, Int. J. Comput. Appl., 151 (2016) 36-43. http://dx.doi.org/10.5120/ijca2016911831

[11] M. V. Rao, B. Mangu, K. S. Kanth, Space vector pulse width modulation control of induction motor, IET-UK, Int. Conf. Electr. Eng. Inform. Commun. Technol. Sci., 2007 (2007) 349 –354. http://dx.doi.org/10.1049/ic:20070636

[12] S. Katyara, A. A. Hashmani, B. S. Chowdhry, Development and Analysis of Pulse Width Modulation Techniques for Induction. Motor. Control. Mehran. Univ. Res. J. Eng. Technol., 39 (2020) 81–96. http://dx.doi.org/10.22581/muet1982.2001.09

[13] I. Bouyakoub, R. Taleb, H. Mellah, A. Zerglaine, Implementation of space vector modulation for two level Three-phase inverter using dSPACE DS1104, Indones. J. Electr. Eng. Comput. Sci., 20 (2020) 744–751. http://dx.doi.org/10.11591/ijeecs.v20.i2.pp744-751

[14] C. Liu . Y. Luo, Overview of advanced control strategies for electric machines, Chinese. J. Electr. Eng., 3 (2019) 53–61. http://dx.doi.org/10.23919/cjee.2017.8048412

[15] Cheng, Quian, Lei Yuan. Vector Control of an Induction Motor based on a DSP, (2011).

[16] K. Sridivya , T. V. Kiran, Space vector PWM control of BLDC motor, Int. Conf. Power Embed, Drive. Control., 2017 (2017) 71–7. http://dx.doi.org/10.1109/ICPEDC.2017.8081062

[17] G. L. Jat, K. Singh, A. Mahajan, S. L. Shimi, Real time speed control of induction motor using new generation DSP controller, 2nd IEEE, Int. Conf. Innov. Appl. Comput. Intell. Power. Energy .Control., with their Impact Humanit. (2016) 90–95. http://dx.doi.org/10.1109/CIPECH.2016.7918744

[18] K. G. Mohammed, Experimental study for enhancement the three-phase induction motor using microprocessor TMS320F, J. Eng. Appl. Sci. 13 (2018) 4771–4775.

[19] T. Tandel, U. Mate, S. Unde, A. Gupta, S. Chaudhary, Speed estimation of induction motor using TMS320F28335 digital signal processor, 2016 IEEE 7th Power India. Int. Conf. , 2016 (2017). http://dx.doi.org/10.1109/POWERI.2016.8077285

[20] C. LUO , Design of Motor Controller Based on TMS320F28335 Digital Signal Processing Chip, DEStech, Trans. Environ. Energy. Earth. Sci., (2019) 352–362. http://dx.doi.org/10.12783/dteees/iccis2019/31685